Direct-excitation cross sections for Cd II low-lying excited states by single-electron impact on Cd atoms

T. Goto, K. Hane, M. Okuda, and S. Hattori
Department of Electronics, Faculty of Engineering, Nagoya University, Nagoya 464, Japan
(Received 23 September 1982)

Emission cross sections for ten spectral lines transiting from Cd II low-lying excited states formed by single-electron impact on Cd atoms have been measured with a photon-counting technique. Polarizations of these lines have also been examined. By the use of these results and removing the influence of cascade transitions, direct-excitation cross sections for seven low-lying states ($5p\ ^2P_{1/2,3/2}$, $5s^2\ ^2D_{3/2,5/2}$, $6s\ ^2S_{1/2}$, $5d\ ^2D_{3/2,5/2}$) have been determined as a function of electron energy. They are found to be of the order of 10^{-17} cm^2 for the $5p$ and $5s^2$ states and of 10^{-18} cm^2 for the $6s$ and $5d$ states at their maxima.

I. INTRODUCTION

Emission cross sections of spectral lines transiting from Cd II excited states formed by single impact between Cd atoms and electrons were measured by several groups.[1–4] (This emission cross section includes the contribution of cascade transitions.) Nevertheless, those results were very different from one another. The values in Ref. 3 are more than ten times as large as those in Ref. 1. Direct-excitation cross sections which do not include the contribution of the cascade transitions have not been investigated as a function of electron energy. Moreover, polarizations of those lines have not been examined.

In the practical positive-column He-Cd$^+$ laser (441.6 nm), it has been demonstrated that the stepwise excitation process [$Cd + e \rightarrow Cd^+ + 2e$ and then $Cd^+ + e \rightarrow (Cd^+)^* + e$ where Cd^+ is the Cd^+ ground-state ion and $(Cd^+)^*$ is the laser-state ion] is the dominant one for the laser states[5–8] and the excitation cross sections for the second process $Cd^+ + e \rightarrow (Cd^+)^* + e$ have already been measured.[9] On the contrary, it has been shown qualitatively that the contribution of the direct-excitation process is small. For the completely quantitative clarification of the positive-column He-Cd$^+$ laser, however, we need also the accurate values of the direct-excitation cross sections for the Cd II excited states. In the hollow-cathode He-Cd$^+$ laser, moreover, it is more necessary to know those values, because there is the report that the direct-excitation process may be important for the laser states.[10]

In this experiment, by using a photon-counting system of high sensitivity controlled by a minicomputer and by obtaining the reliable value of the Cd-atom density with an absorption method, the emission cross sections for the Cd II spectral lines shown in Fig. 1 have been measured accurately in the electron-energy region of 10 to 200 eV. The polarizations of those lines have also been examined. By using those results, the direct-excitation cross sections for seven Cd II excited states

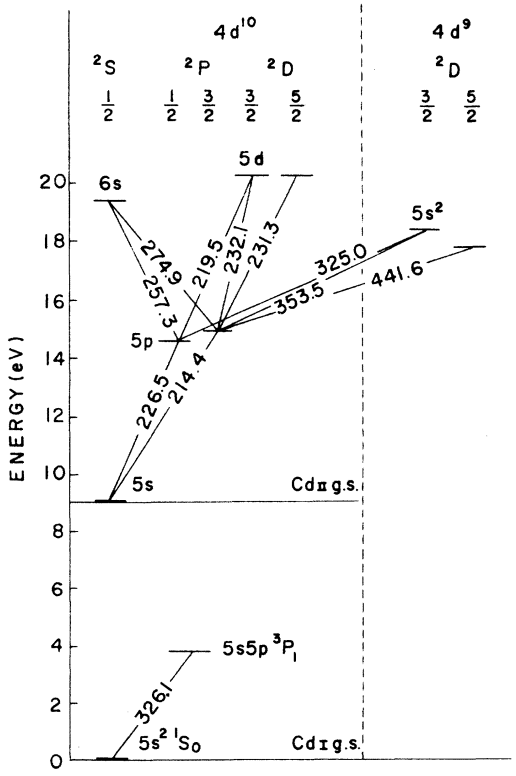

FIG. 1. Energy-level diagram of Cd I and Cd II. Cd I 326.1-nm line was used for the absorption measurement.

($5p\,^2P_{1/2,3/2}$, $5s^2\,^2D_{3/2,5/2}$, $6s\,^2S_{1/2}$, $5d\,^2D_{3/2,5/2}$) have been determined as a function of electron energy.

II. EXPERIMENTAL APPARATUS AND MEASUREMENT METHOD

A. General

When we bombard Cd atoms with electrons at very low Cd vapor pressures, Cd atoms are excited to various Cd II states by single-electron impact and photons of spectral lines transiting from those states are emitted. In this case, if the Cd-atom density is uniform in the collision volume, the emission cross section Q_{ij} for the spectral line of a wavelength λ_{ij} transiting from the state i to the state j is given by

$$Q_{ij}=(1-\tfrac{1}{3}P_{ij})\frac{S_{ij}e}{N_{\mathrm{Cd}}I_e dD_{ij}}, \tag{1}$$

where S_{ij} is the recorded photon count rate of the spectral line λ_{ij}, e is the electric charge, N_{Cd} is the Cd-atom density, I_e is the total electron current, D_{ij} is the absolute sensitivity of the optical detection system at the wavelength λ_{ij}, and d is the length of the collision volume. P_{ij} is the polarization fraction and is given by

$$P_{ij}=\frac{I_{\parallel}-I_{\perp}}{I_{\parallel}+I_{\perp}}, \tag{2}$$

where $I_{\parallel}$ and $I_{\perp}$ are the calibrated photon-count rates of the components polarized parallel and perpendicular to the direction of the electron beam, respectively.

The direct-excitation cross section σ_i for the state i is obtained from the relation

$$\sigma_i=\sum_j Q_{ij}-\sum_k Q_{ki}, \tag{3}$$

where Q_{ki} is the emission cross section for a cascade transition from the state k to the state i.

B. Apparatus

Figure 2 shows the block diagram of experimental apparatus. An excitation part is placed at the center of a vacuum chamber of 450-mm diameter, which is evacuated to a pressure of 10^{-8} Torr. The structure of the excitation part when we view it standing at the position AA is shown in the upper right-hand corner of Fig. 2. An electron source has an oxide cathode and three grids: focusing aperture electrode, accelerating grid, and beam control grid. The extracted electron beam is limited by an aperture of 2-mm diameter. After this electron beam crosses the collision volume, it is collected by an electron Faraday cup which is maintained at the positive potential with respect to the ground potential. The typical electron beam current was 30 to 900 μA in the acceleration energy region of 20 to 200 eV. The energy spread of the electron beam was estimated to be less than 1.5 eV. On the other hand, Cd atoms are evaporated from the Cd crucible by a heater, diffuse into the collision volume, and are crossed by the electron beam. This collision volume is the cylindrical shape of about 2-mm diameter and 9-mm height. The Cd atoms are excited to various states by single-electron impact there, and emit photons. They are observed along the third orthogonal axis by the optical detection system.

The detection system consists of a window of the vacuum chamber, a monochromator (Nikon G-250 model) with a dispersion of 3 nm/mm, a photomultiplier tube manufactured for a photon-counting process (with noise of a few counts per second), and a photon-counting system including a preamplifier, a pulse shaper, and a binary counter. The background noise is removed by the modulation of the electron beam and the signal counts in phase with the electron beam are accumulated in the memories of a minicomputer. The modulation scheme was the square wave one and its period was 200 msec in the present experiment. The signal count was accumulated until the standard deviation $s(\sqrt{S+N})$ due to the Poisson statistics of the total count $S+N$ was reduced to less than 1% or 2% of the accumulated signal count S, where S and N are the signal and noise counts, respectively, accumulated during the measuring time. The photon-counting system, the beam modulation system, and the electron-energy regulator all are controlled by the computer, and the electron current collected by the Faraday cup is read by the computer.

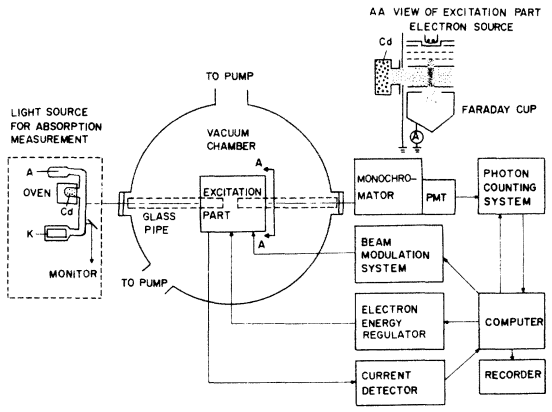

FIG. 2. Block diagram of the experimental apparatus. He-Cd tube and the two glass pipes drawn by broken lines were inserted into the position shown in the figure, only for measuring the Cd-atom density with the absorption method.

C. Measurement method for the emission cross sections

The emission cross sections of the ten Cd II spectral lines as a function of electron energy were obtained in the following four procedures: (i) the measurement of the optical excitation function of each line between the threshold energy and 200 eV, (ii) that of the polarization fraction P_{ij}, (iii) that of the relative emission cross sections for the ten lines at the electron energy of 50 eV, and (iv) that of the absolute emission cross section for the 441.6-nm line at the electron energy of 50 eV. The measurements (i) to (iii) were made in the Cd vapor pressure region of 10^{-5} Torr or less where only the single-electron impact was certain to occur as a collision process. The measurement (iv) was made in the slightly higher Cd vapor pressure region.

(i) Each optical excitation function was obtained by measuring the signal count rate divided by the electron current (S_{ij}/I_e) as a function of electron energy under a constant Cd vapor pressure. The electron energy was varied from 10 to 200 eV with a step of 2 eV and the measurement time was less than one hour. It was confirmed by monitoring the 274.9-nm photon-count rate that the Cd-atom density was almost constant during the measurement of one hour. It was also confirmed that the optical excitation function was independent of the Cd vapor pressure under the present conditions.

(ii) The values of the polarization fractions P_{ij} of the lines were obtained by measuring $I_{||}$ and $I_{\perp}$ in Eq. (2) as a function of electron energy with a polarizer of calcite. Here the sensitivities of the optical detection system for the parallel and perpendicular components were calibrated with a tungsten lamp and a deutrium lamp.

(iii) The relative emission cross sections were obtained by measuring the photon-count rates for the ten lines at the electron energy of 50 eV and dividing them by the relative values of D_{ij} in Eq. (1). The relative variation of D_{ij} with wavelength was measured carefully and repeatedly by using the tungsten standard lamp and the deutrium lamp in the regions of 300 to 600 nm and 190 to 400 nm, respectively. This measurement was made by removing the excitation part and placing the lamp just at the position of the collision volume in the chamber. In the region of 300 to 400 nm, the results for the two lamps agreed well with each other. The uncertainty of this relative calibration was estimated to be about $\pm 3.5\%$ in the region of 200 to 600 nm. (The signal due to the stray light at the infrared wavelengths was estimated to be $\pm 1\%$ or less.)

(iv) To determine the absolute emission cross section Q_{ij} for the 441.6-nm line, N_{Cd} and the absolute value of D_{ij} in Eq. (1) must be known accurately. The N_{Cd} was obtained by measuring the absorption coefficient of the Cd I 326.1-nm line with an absorption method. The brief description of the method is given below. As a light source, the positive-column He-Cd discharge tube of 3.5-mm diameter was used. It was placed at the position drawn in Fig. 2. The Cd-atom density in the tube was about 5×10^{12} cm^{-3}. Therefore, the 326.1-nm line taken out of the side of the tube was not self-absorbed and its profile $f(\nu)$ was the superposition of the isotope shift components each of which had the Doppler width corresponding to a gas temperature of 600 K. The photon-count rates S_1 and S_2 for the 326.1-nm line were measured before and after warming up the Cd crucible (that is, without and with Cd vapor in the collision volume), respectively. The ratio S_2/S_1 is given by

$$G(k_0 l)=\frac{S_2}{S_1}=\frac{\int_0^{\infty} f(\nu)\exp[-k_0 l g(\nu)]d\nu}{\int_0^{\infty} f(\nu)d\nu}, \tag{4}$$

where $k_0 l$ is the absorption coefficient at a certain frequency within the line profile, l is the length of the absorption region, and $g(\nu)$ is the absorption profile of the Cd I 326.1-nm line by Cd atoms in the collision volume which was nearly equal to $f(\nu)$ in the present experiment. This $G(k_0 l)$ can be calculated as a function of $k_0 l$ easily. The Cd-atom density N_{Cd} is given by

$$N_{\mathrm{Cd}}=\left[8\pi g_1 k_0 l\int_0^{\infty} g(\nu)d\nu\right]\Big/(\lambda_0^2 g_2 A l), \tag{5}$$

where g_2 and g_1 are the statistical weights for the upper and lower states of the 326.1-nm line, respectively, λ_0 is the wavelength, and A is the transition probability of the 326.1-nm line. Therefore, from the measured S_2/S_1 and the computed $G(k_0 l)$ versus $k_0 l$ curve, N_{Cd} could be obtained. When Cd vapor floats between two windows of the vaccum chamber and the collision volume in the excitation part, we cannot measure N_{Cd} in the collision volume accurately. To minimize this uncertainty, the two glass pipes with enclosed ends were placed between the two windows and the collision volume (shown by the broken lines) so that the 326.1-nm photons could be absorbed only by Cd atoms in the collision volume. These pipes were heated so that Cd atoms should not contaminate the ends. Throughout the measurement of $G(k_0 l)$, the intensity of the 326.1-nm line emitted from the light source was monitored with another detection apparatus and the uncertainty due to its fluctuation was removed. The uncertainty of the measured N_{Cd} was estimated

to be about ±20%. The measurement of S_{ij} for the 441.6-nm line and N_{Cd} was carried out at several Cd vapor pressures of the order of 10^{-4} Torr or less and S_{ij}/N_{Cd} was determined at the electron energy of 50 eV under the existence of the glass pipes. The absolute value of D_{ij} at 441.6 nm was obtained in the same way as described in Ref. 9, that is, by using a light emitting diode the absolute intensity of which was calibrated previously. The obtained value of D_{ij} was 6.4×10^{-6} at 441.6 nm. The uncertainty due to this calibration was estimated to be ±12%. The absolute value of Q_{ij} for the 441.6-nm line at the electron energy of 50 eV was determined by substituting the measured S_{ij}/N_{Cd}, D_{ij}, P_{ij}, and I_e into Eq. (1).

The absolute emission cross sections for the ten lines as a function of electron energy were obtained by combining the results of (i) to (iv).

III. RESULTS AND DISCUSSION

Figure 3 shows the photon-count rate S_{ij} for the 441.6-nm line at the electron energy of 50 eV as a function of N_{Cd}. The S_{ij} increases nearly linearly with N_{Cd}. This means that some additional processes other than single-electron impact could be negligible in this N_{Cd} region (the order of 10^{-4} Torr or less). With the use of the slope S_{ij}/N_{Cd} obtained from Fig. 3 and the measured D_{ij}, P_{ij}, and I_e, the absolute emission cross section for the 441.6-nm line was determined to be 3.8×10^{-17} cm^2 at the electron energy of 50 eV. The uncertainty of this absolute value was evaluated to be ±24% when combined in quadrature.

Figure 4 shows the polarization fractions P_{ij} as a function of electron energy for the 441.6-, 325.0-, 214.4-, 226.5-, 274.9-, and 231.3-nm lines. In the present electron-energy region, the measured polarization fraction of any line is between 0.1 and −0.1, and is almost constant although those for the 214.4- and 325.0-nm lines appear to change somewhat below 50 eV. Therefore, the influence of P_{ij} on Q_{ij} is less than ±3%.

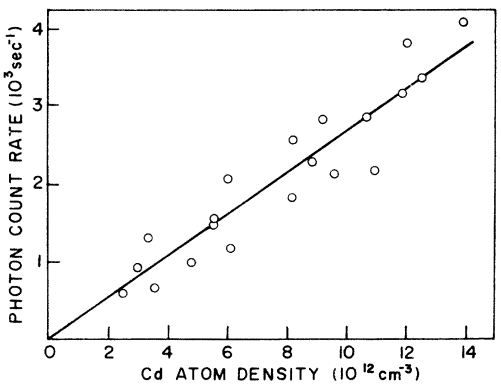

FIG. 3. Photon-count rate S_{ij} for the 441.6-nm line vs the Cd-atom density N_{Cd} at an electron energy of 50 eV.

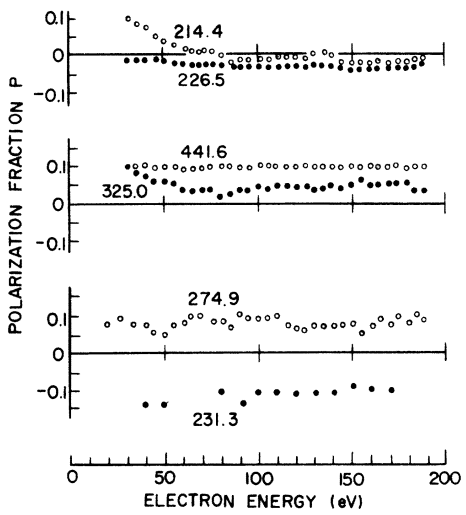

FIG. 4. Polarization fraction P_{ij} as a function of electron energy.

Figure 5 shows the emission cross sections Q_{ij} for the 214.4-, 226.5-, 441.6-, 325.0-, and 353.5-nm lines as a function of electron energy. For each optical excitation function, the standard deviation s of the accumulated signal count, which is the main uncertainty of the optical excitation function, is less than 1% above 30 eV. The uncertainty ϵ_r of the relative value of the emission cross section in the figure is evaluated by combining in quadrature the value of s

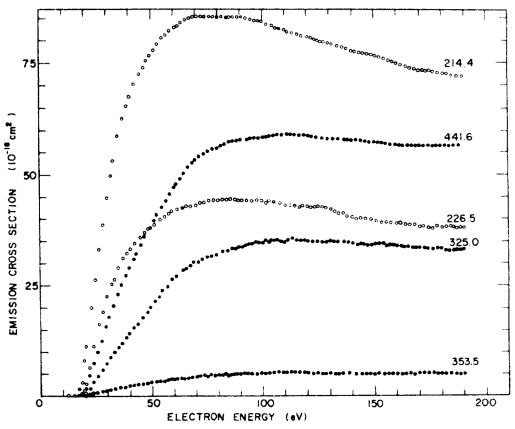

FIG. 5. Emission cross sections Q_{ij} for the 214.4-, 226.5-, 441.6-, 325.0-, and 353.5-nm lines as a function of electron energy. Standard deviation s of each data point is 0.5% for the first four lines and 1.5% for the 353.5-nm line in the electron-energy region of 30 to 200 eV.

and the uncertainty of the relative values of D_{ij}. The obtained ϵ_r is $\pm 3.6\%$. The Q_{ij} for the 214.4- and 226.5-nm lines increase in the region of threshold to 70 eV and then decrease somewhat. Those for the 441.6-, 325.0-, and 353.5-nm lines are very similar in their relative variations. They increase in the region of threshold to about 90 eV but are almost constant above 90 eV.

Figure 6 shows the emission cross sections for the 274.9-, 257.3-, 231.3-, 219.5-, and 232.1-nm lines as a function of electron energy. The value of s for each optical excitation function is less than 2% above 30 eV. The value of ϵ_r of the emission cross section is $\pm 4\%$. The obtained Q_{ij} all have clear maxima around 50 eV and then decrease to about 25% of the peak values at 190 eV, being different from the lines shown in Fig. 5.

The Q_{ij} were measured for four lines in Ref. 1, ten lines in Ref. 2, only one line in Ref. 3, and three lines in Ref. 4 among ten lines shown in Fig. 1. The relative changes of the Q_{ij} in them agrees qualitatively with the present ones, but the decreases in the higher-energy region are less than the present ones. The uncertainties included in the zero-signal levels might have been large because the photon-counting systems of the high sensitivity were not used in those experiments and additional processes might have been included somewhat because the Cd vapor pressures were relatively high. Possibly they can cause the lesser decrease in the higher-energy region. The absolute values of the Q_{ij} in Ref. 2 agree within a factor of 2 with the present ones but those in Refs.

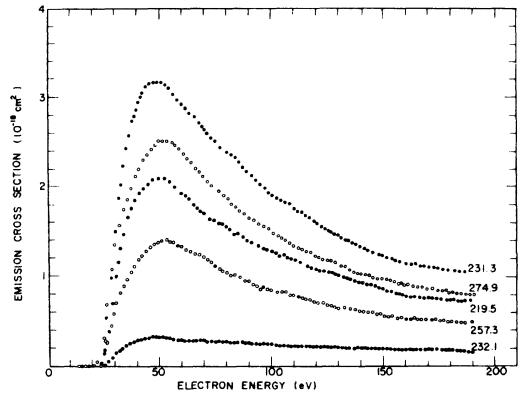

FIG. 6. Emission cross sections Q_{ij} for the 274.9-, 257.3-, 231.3-, 219.5-, and 232.1-nm lines as a function of electron energy. Standard deviation s of each data point is 0.9% for the 274.9-nm line and 1.8% for the other lines in the electron-energy region of 30 to 200 eV.

1 and 3 are very different from the present ones. They were probably due to the fact that N_{Cd} were obtained directly with the absorption method in the present experiment and Ref. 2 but were deduced from the temperatures of the Cd crucibles in Refs. 1 and 3. Sometimes the N_{Cd} deduced from the oven temperature include a very large uncertainty.

Figure 7 shows the direct excitation cross sections σ_i for the $5p$ and $5s^2$ states as a function of the electron energy, which were obtained using the results

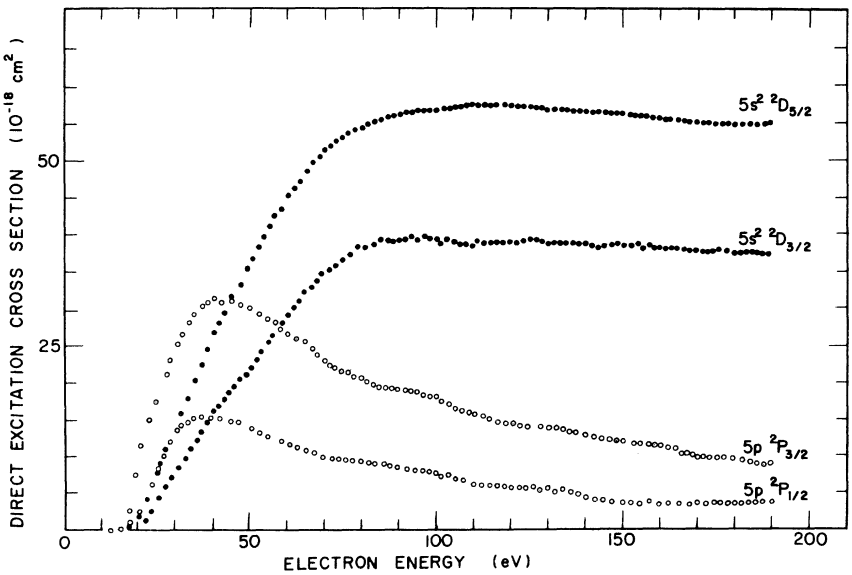

FIG. 7. Direct-excitation cross sections σ_i for the $5p\ ^2P_{3/2,1/2}$ and $5s^2\,^2D_{5/2,3/2}$ states as a function of electron energy. Uncertainty ϵ_{rd} involved in the relative values is about $\pm 20\%$ for the $5p\ ^2P$ states and $\pm 4\%$ for the $5s^2\,^2D$ states.

shown in Figs. 5 and 6.

The value of σ_i for the $5p\,^2P_{3/2}$ state was obtained by subtracting the sum of the Q_{ki} for the five cascade lines (441.6, 353.5, 231.3, 232.1, and 274.9 nm) from the Q_{ij} for the 214.4-nm line. That of σ_i for the $5p\,^2P_{1/2}$ state was obtained by subtracting the sum of the Q_{ik} for the three lines (325.0, 219.5, and 257.3 nm) from the Q_{ij} for the 226.5-nm line. Since other cascade transitions are weak compared with the 441.6-nm line, etc., they are completely negligible. For any of the $5p\,^2P_{1/2,3/2}$ states, the resultant σ_i is different from Q_i in its absolute value and relative variation. σ_i is rather smaller than Q_{ij} and has a maximum around 40 eV. The relative variation of σ_i is similar to those for the $5d$ and $6s$ states to be shown in Fig. 8. The uncertainty ϵ_{rd} of the relative value of σ_i is evaluated to be about $\pm 20\%$ which is much larger than that of Q_{ij}. This is caused by the quite large contribution of the cascade transitions.

On the other hand, the ionic Beutler ground states $5s^2\,^2D_{5/2}$ and $5s^2\,^2D_{3/2}$ have many, but weak, cascade transitions. In another experiment we measured their emission cross sections as a function of electron energy.[11] Those results were used here and σ_i for the $5s^2$ states in Fig. 7 were obtained. The contributions of the cascade transitions to Q_{ij} were very small being different from the $5p$ states, for example, 5% for the $5s^2\,^2D_{5/2}$ state and 2.5% for the $5s^2\,^2D_{3/2}$ state at the electron energy of 50 eV. Therefore, for any of the $5s^2\,^2D_{3/2,5/2}$ states, σ_i is very close to Q_{ij} in its absolute value and relative variation, and the ϵ_{rd} of σ_i is about $\pm 3.6\%$. It is to be noted that σ_i for the $5s^2$ states are rather larger than σ_i for the $5p$ states, particularly in the region above 50 eV.

It would be expected that the $5s^2\,^2D$ states are formed almost exclusively by the removal of a single inner-shell electron (one of the $4d^{10}$ electrons) while the ordinary $5p$, $5d$, and $6s$ states are formed by ionization of one electron and excitation of another electron. In fact, the shape of the $5s^2\,^2D$ excitation cross section should be that normally ascribed to ionization, and the simple Lotz's prediction[12] for the ionization gives a cross section even greater than the sum of the excitation cross sections of the $5s^2\,^2D$ states deduced from the emission measurements, although Lotz's equation does not give the quantitative estimate for the Cd atoms. Therefore, it is possible that the cross sections for the formation of the $5s^2\,^2D$ states are rather larger than those for the other states.

Figure 8 shows the direct-excitation cross sections σ_i for the $5d\,^2D_{3/2,5/2}$ and $6s\,^2S_{1/2}$ states as a function of electron energy. As to the main cascade transition to these states, the results obtained in our other experiment were used.[11] For any of the $5d\,^2D_{3/2,5/2}$ states the contribution of the cascade transitions to Q_{ij} was about 30% at the electron energy of 50 eV. The obtained σ_i is 0.7 times as large as Q_{ij} and the shape of σ_i is similar to that of Q_{ij}. For the $6s\,^2S_{1/2}$ state, the strongest cascade transition is the 806.7-nm line from the $6p\,^2P_{3/2}$ state. σ_i was obtained by subtracting Q_{ij} for the 806.7-nm line from the sum of Q_{ij} for the 274.9- and 257.3-nm lines. The ϵ_{rd} of σ_i is about $\pm 5\%$ for any of $5d\,^2D_{3/2,5/2}$ and $6s\,^2S_{1/2}$ states.

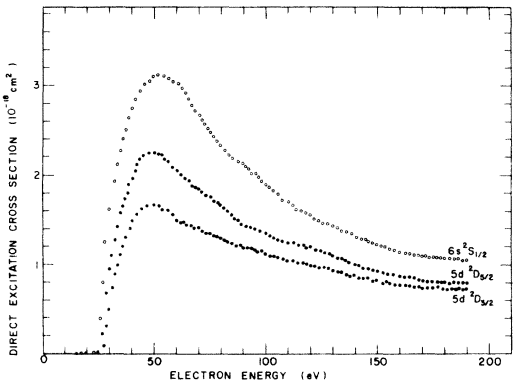

FIG. 8. Direct-excitation cross sections σ_i for the $5d\,^2D_{5/2,3/2}$ and $6s\,^2S_{1/2}$ states as a function of electron energy. Uncertainty ϵ_{rd} involved in the relative values is about $\pm 5\%$.

In this experiment, the absolute values of all Q_{ij} and σ_i were determined on the basis of Q_{ij} for the 441.6-nm line stated in procedure iv of Sec. II C. Therefore, the uncertainty of the absolute value for each cross section is obtained by combining in quadrature the uncertainty $\pm 24\%$ of Q_{ij} for the 441.6-nm line and the uncertainty of the relative value (ϵ_r or ϵ_{rd}).

By the present experiment, it has been shown that σ_i for the ionic Beutler ground states $5s^2$ are very large in magnitude and have the singular relative variations which are different from σ_i for the $4d^{10}5p$, $6s$, and $5d$ states.

In the positive-column He-Cd $^+$ laser described in Ref. 5, the direct-excitation rate estimated using the present result has been only a few percent of the stepwise-excitation rate. Therefore, the present result does not change our previous conclusion that the stepwise-excitation process is the dominant one, but it has become possible to estimate the direct-excitation rate quantitatively in the positive-column He-Cd$^+$ laser, and also in the hollow-cathode He-Cd$^+$ laser if various particle densities are measured accurately.

ACKNOWLEDGMENT

This work was supported by Grant-in-Aid for Co-operative Research of the Ministry of Education.

[1]R. J. Anderson and E. T. P. Lee, J. Chem. Phys. 53, 754 (1970).
[2]S. P. Varshavskii, A. A. Mityureva, and N. P. Penkin, Opt. Spectrosc. 29, 341 (1970).
[3]V. S. Aleinikov and V. V. Vshakov, Opt. Spectrosc. 29, 111 (1970).
[4]I. P. Bogdanova, S. V. Ryazantseva, and V. E. Yakhontova, Opt. Spectrosc. 45, 622 (1978).
[5]M. Mori, M. Murayama, T. Goto, and S. Hattori, IEEE J. Quantum Electron. QE-14, 427 (1978).
[6]T. Goto, J. Phys. D 14, 575 (1981).
[7]T. Goto, K. Hane, and S. Hattori, J. Phys. D 14, 587 (1981).
[8]T. Goto, J. Phys. D 15, 421 (1982).
[9]K. Hane, T. Goto, and S. Hattori, Phys. Rev. A 27, 124 (1983).
[10]A. I. McIntosh and J. R. Grace, Aust. J. Phys. 32, 561 (1979).
[11]The results are planned to be reported in another paper by us.
[12]W. Lotz, J. Phys. 220, 466 (1969).